The Astrophysical Journal Letters, 786:L22 (6pp), 2014 May 10 doi:10.1088/2041-8205/786/2/L22

PENUMBRAL-LIKE FILAMENTS IN THE SOLAR PHOTOSPHERE AS A MANIFESTATION OF FLUX EMERGENCE

Salvo L. Guglielmino[1], Francesca Zuccarello[1], and Paolo Romano[2]
[1] Dipartimento di Fisica e Astronomia, Università di Catania, Via S. Sofia 78, I-95123 Catania, Italy; sgu@oact.inaf.it
[2] INAF–Osservatorio Astrofisico di Catania, Via S. Sofia 78, I-95123 Catania, Italy
Received 2013 October 25; accepted 2014 February 18; published 2014 April 24

ABSTRACT

Rare observations of the solar photosphere show the appearance of *orphan penumbrae*, filamentary structures very similar to a bundle of sunspot penumbral filaments not connected to any umbra. Lim et al. found an orphan penumbra in active region NOAA 11391 near a mature sunspot. We analyze a different data set to study the same structure using the Solar Optical Telescope on board the *Hinode* satellite. Spectropolarimetric measurements along the Fe I 630.2 nm pair, complemented by *G*-band and Ca II H filtergrams, show the evolution of this penumbral-like structure and reveal that an emerging flux region is its ancestor. We find new evidence for the interaction between the emerging flux and the pre-existing field that leads to a brightening observed near the base of the chromosphere. Our analysis suggests that as a result of the combination of photospheric flux emergence and magneto-convection in inclined fields the horizontal component of the emerging field can be trapped in the photosphere by the overlying fields and form a structure resembling penumbral filaments.

Key words: Sun: magnetic fields – Sun: photosphere – sunspots – techniques: high angular resolution – techniques: polarimetric

1. INTRODUCTION

Orphan penumbrae (Zirin & Wang 1991) are filamentary structures rarely observed in the solar photosphere that are very similar to a bundle of penumbral filaments but are not spreading out from any sunspot umbra. Observations carried out with increasing spatial resolution (Zirin & Wang 1991; Denker et al. 1997; Kuckein et al. 2012a, 2012b; Lim et al. 2013; Jurčák et al. 2014; Zuccarello et al. 2014) show that they have many characteristics of normal penumbrae surrounding sunspot umbrae in solar active regions (ARs): a fibrilar "uncombed" structure, a bolometric brightness of about 80% of the undisturbed quiet Sun continuum intensity, and similar plasma motions. However, they usually have a shorter lifetime than normal penumbrae and do not possess a counterpart in the chromosphere.

The origin of these structures is still controversial and appears to be somehow related to the formation process of regular penumbrae (Zuccarello et al. 2014). Flux emergence seems to be an important element in this process. Leka & Skumanich (1998) suggested that emerging, horizontal field lines could be trapped and form a penumbra rather than continuing to rise to higher layers when a magnetic canopy overlays the emerging region. The role played by the presence of such a magnetic canopy at the chromospheric level in penumbral formation was confirmed by Ca II line observations carried out by Shimizu et al. (2012) and Romano et al. (2013, 2014).

A number of MHD theoretical models deal with penumbral formation (see, e.g., Schlichenmaier 2009; Rempel & Schlichenmaier 2011). Recent numerical simulations of radiative magneto-convection in inclined fields (Rempel et al. 2009; Rempel 2011) stressed the importance of the magnetic field topology and velocity fields in the lower chromosphere and upper photosphere during this process. Rempel (2012) showed that penumbral formation is favored when the horizontal field component is enhanced at the top of the computational domain. This finding suggests that the presence of an inclined canopy in the atmosphere may be crucial for the development of penumbrae.

Recently, Lim et al. (2013) reported on the presence of an orphan penumbra near a mature sunspot in AR NOAA 11391. Images acquired at high spatial resolution (0.″11) with the New Solar Telescope, using a broadband TiO filter (705.7 nm), reveal that this orphan penumbra connects two tiny dark points. Cospatial, simultaneous filtergrams taken in the blue wing of Hα line (−75 pm) show that low-lying chromospheric fibrils, which indicate canopy fields, overlay the orphan penumbra. One of the TiO dark points appears as an Hα bright patch. Lim et al. (2013) have interpreted this orphan penumbra as the upper horizontal part of an emerging Ω loop, trapped in the photosphere by the overlying canopy fields. However, it is quite difficult to consider this result to be well assessed, relying only on information from the monochromatic, single-time observations presented by the authors without any simultaneous spectroscopic and/or spectropolarimetric measurements.

In this Letter we study this penumbral-like structure present in AR NOAA 11391, using multi-wavelength, high-resolution observations acquired by the *Hinode* satellite (Kosugi et al. 2007). We complement the analysis of Lim et al. (2013) showing the evolution of the structure. In particular, through the analysis of spectropolarimetric measurements we reveal the dynamics and the magnetic configuration of this region and provide an explanation for the formation of the penumbral-like filaments. In Section 2, we describe the observations; Section 3 reports on the evolution of the structure and its magnetic configuration; and in Section 4 we discuss our findings.

2. OBSERVATIONS AND DATA ANALYSIS

The Solar Optical Telescope (SOT; Tsuneta et al. 2008) aboard the *Hinode* satellite observed AR NOAA 11391 for about 56 hr, starting from 2012 January 10 at 15:34 UT. In this work we analyze data acquired during the interval 15:34 UT on January 10–02:07 UT on January 11, during which the penumbral-like structure was observed, initially located at solar coordinates [200″, 225″] (μ = 0.95). Note that our observations overlap

those shown by Lim et al. (2013), taken at 18:55 UT (see their Figure 3, panels (C) and (D)).

At that time, the SOT spectropolarimeter (SP) performed two raster scans over the AR, begun at 15:34:08 UT and 18:35:05 UT, respectively, each with a duration of 63 minutes. Full Stokes parameters were acquired along the Fe I line pair at 630.2 nm, with a pixel size of 0.″32 and a field of view (FoV) of about $297'' \times 164''$.

Simultaneously, the SOT Broadband Filter Imager (BFI/FG) acquired a series of filtergrams in the *G* band (430.5 ± 0.8 nm) and in the core of the Ca II H line (396.85 ± 0.3 nm). These images cover a FoV of $188.''3 \times 111.''6$, with a pixel size of 0.″109. The cadence of these data is 45 minutes for *G*-band filtergrams and three minutes for Ca II H images, with a gap in the acquisition between 17:41 UT and 18:36 UT.

All the SOT/SP–FG data have been corrected for dark current, flat field, and cosmic rays using the standard IDL *SolarSoft* routines.

The SOT/SP continuum intensity I_c in each scan has been normalized to the value of the intensity of a large area of undisturbed quiet Sun present in the upper and lower parts of the full FoV. The maps of the physical parameters have been obtained from the standard Milne–Eddington (M-E) CSAC inversions, which use the MERLIN inversion code. The least-squares fitting of the Stokes profiles retrieves the magnetic field strength, inclination and azimuth angles, line-of-sight (LOS) velocity, line strength, line broadening, and magnetic filling factor. All of these parameters are considered constant in the atmosphere.

The sequence of SOT/FG *G*-band filtergrams has been aligned to the first image in time by using the IDL routine *fg_rigidalign*, considering a square of 320×320 pixels over the large sunspot present in the FoV as a reference. SOT/FG Ca II H images, also aligned between each other with rigid displacements, have been aligned to the *G*-band filtergram series, according to the information provided by Shimizu et al. (2007) about the SOT internal offset.

The SOT/SP continuum images have been cross-correlated with the SOT/FG *G*-band filtergrams closest in time with respect to the acquisition time of the central slit of each scan, taking into account the drift of the image center due to the solar differential rotation. In order to obtain precise pointing information, as a reference, we have also used a full-disk continuum image in the Fe I line at (617.3 nm), with a pixel size 0.″504, acquired at 18:37:10 UT by the Helioseismic and Magnetic Imager (HMI; Schou et al. 2012) on board the *SDO* satellite (Pesnell et al. 2012). We have obtained the displacement between this *SDO* image and the simultaneous SOT/FG *G*-band filtergram with cross-correlation techniques, taking into account the different pixel sizes.

The 180° azimuth ambiguity has been solved by applying the Non-Potential Field Calculation (Georgoulis 2005) code over the entire FoV of SOT/SP scans, taking into account the correction for the magnetic filling factor. This code has also performed the transformation of the components of the vector magnetic field into the local solar frame. LOS velocities resulting from the M-E inversion have been calibrated assuming that plasma in sunspot umbrae ($I_c < 0.5$) is globally at rest.

3. RESULTS

Figure 1 shows that the penumbral-like structure is located near the southeastern edge of the large leading sunspot of AR NOAA 11391 that has been observed on the photosphere since

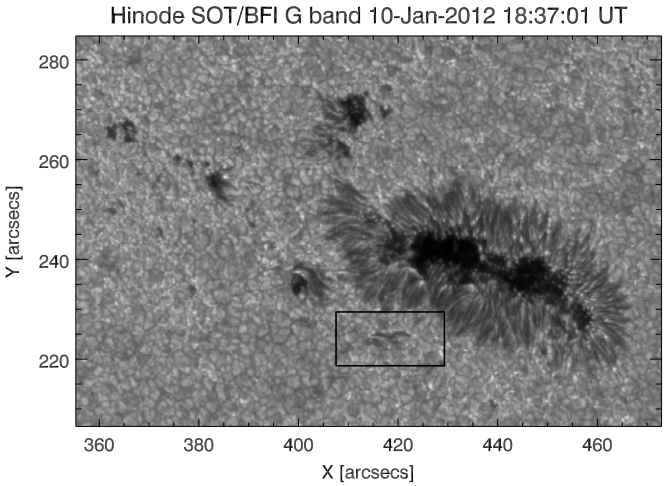

Figure 1. *Hinode* SOT/FG map showing the western part of AR NOAA 11391 observed in the *G* band. The box, with an FoV of about $22'' \times 11''$, frames the penumbral-like structure. Solar north is on top, west is on the right.

the appearance of the AR on the solar disk, which occurred on January 3.

Figure 2 displays a sequence of *G*-band filtergrams, with 90 minute cadence, of the partial FoV indicated in the black box of Figure 1. The evolution shown in Figure 2 points out that at the beginning of *Hinode* observations (15:36 UT) there are two small pores that are aligned along a direction tilted at about 45° with respect to the solar east–west direction. At 17:06 UT, the two pores distance each other and are aligned along a less tilted direction. A fibrilar structure develops in the region between these two pores, connecting them, and from that moment on the pores are no longer observed. The remaining fibrilar structure, which has grown and filled the region, is then recognized as the orphan penumbra by Lim et al. (2013), with the filaments aligned along the solar east–west direction (18:37 UT). At first, these fibrils seem to fade (20:07 UT), but a new bundle of filaments is later formed on the eastern part of the patch (21:37 UT), showing a different tilt angle with respect to the east–west direction, as compared to the structure observed before. This structure shrinks (23:07–00:47 UT) and finally vanishes (02:07 UT).

Note that the pores and later the penumbral-like filaments remain behind the leading sunspot, tracked by the alignment algorithm, which moves westward with higher velocity. This is easily deduced from the displacements of the white crosses, increasing eastward in Figure 2, that indicate the position of the center of mass of the structures. This has been calculated by considering the centroid of those pixels in the regions that have *G*-band intensity values, normalized to a quiet Sun portion adjacent in the FoV, below 0.9.

The maps of the physical parameters obtained from SOT/SP measurements, shown in Figures 3 and 4, shed light on the nature of this phenomenon. At 16:02 UT (see Figure 3), the two pores coincide with two magnetic flux concentrations of opposite polarity, with total flux content of about 7×10^{19} Mx. The darkest regions, with $I_c < 0.7$, correspond to nearly vertical field lines, with an average inclination angle, measured with respect to the normal to the solar photosphere, of 15° and 160° for the positive- and negative-polarity pore, respectively. The 2″-width region around [13″, 5″] (see the box in Figure 3) is characterized by highly inclined fields, nearly parallel to the photosphere, with an average horizontal component of 650 G, up

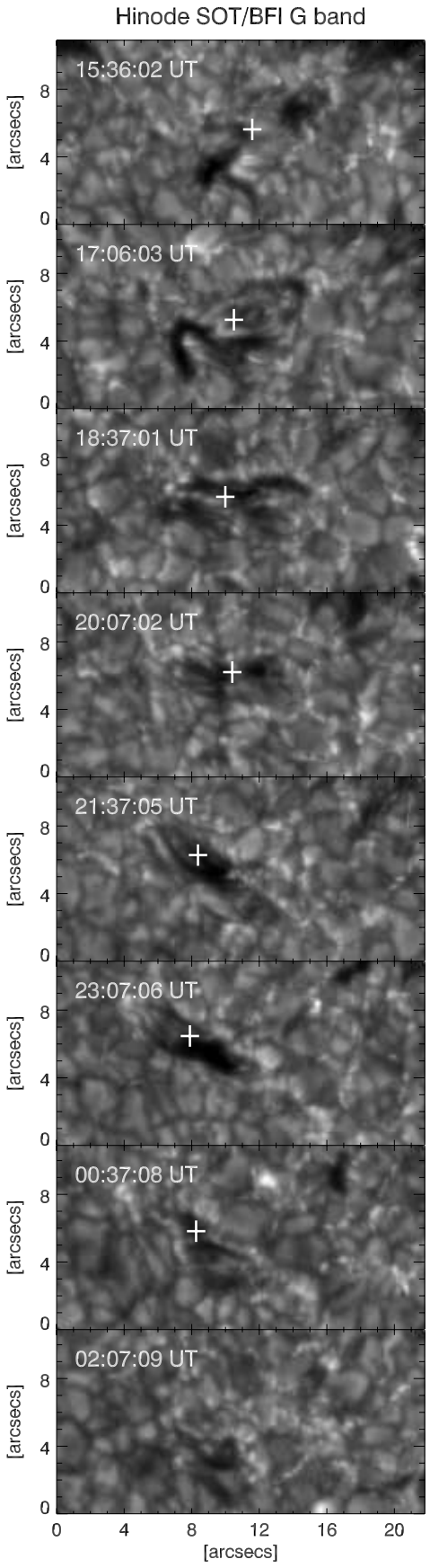

Figure 2. Sequence of SOT/FG *G*-band filtergrams for the subFoV indicated in Figure 1, from 15:36 UT on January 10 to 02:07 UT on January 11. Images are rescaled to the minimum and maximum intensity of the entire sequence. White crosses indicate the position of the center of mass of the structure in each frame.

to 900 G. The azimuth angle is quite homogeneous and the field lines point in the direction from the positive-polarity pore to the negative-polarity pore. This zone in between the pores also exhibits upward motions with an average velocity of $-0.9\,\mathrm{km\,s^{-1}}$. Such characteristics identify this region as an emergence zone (Lites et al. 1998).

During the second scan, shown in Figure 4, when the penumbral-like filaments have already formed, the magnetic flux content of the whole structure is about 6×10^{19} Mx. The regions with $I_c < 0.7$ have become smaller and no longer coincide with the areas that have the most vertical fields. The total magnetic field has a mean value of ∼1000 G within the contour corresponding to $I_c = 0.9$. The horizontal component of the field, roughly aligned in the solar east–west direction and not everywhere orthogonal to the *S*-shaped neutral line, is comparable with that measured during the first scan on average, with a peak of 1000 G. Interestingly, the LOS velocity shows a peculiar behavior along the neutral line, where it has stronger values up to $\pm 2\,\mathrm{km\,s^{-1}}$. This result is not an artifact of the M-E inversion, as it is also visible in Doppler shift maps for both the lines of the Fe I 630.2 nm pair, obtained from a Gaussian fit of the Stokes *I* profile only. In this case the highest velocity values are slightly lower.

Figure 5 shows a sequence of Ca II H images with 12 minutes cadence. Due to the large photospheric contribution included in the passband of the SOT/BFI Ca II H filter (Carlsson et al. 2007), it is possible to observe fibrilar structures extending in the photosphere over the region.

We notice a brightness enhancement located at [7″, 7″], corresponding with the northeastern border of the penumbral-like region. It has a duration of about 30 minutes. A peak of a factor of three, with respect to the quiet level, is estimated by averaging the Ca II H signal over the left half of the subFoV at 18:39 UT, which occurs between 19:03 UT and 19:15 UT. This brightening region has a lengthwise extent of 1″ and spatially coincides with the contact zone between the positive patch of the penumbral-like structure and the diffuse, negative field of the plage near the sunspot (see Figure 4, third and fifth panels). The *G*-band filtergram acquired during this Ca II H sequence does not show any similar brightenings.

4. CONCLUSIONS

The overall description of the photospheric evolution and magnetic configuration of the penumbral-like structure is consistent with the emergence and subsequent decay of a relatively large ephemeral region (Harvey & Martin 1973). Thus, the region with upflowing, horizontal fields in between the pores seen at 16:02 UT is the emergence zone of the emerging bipole. As its total flux content exceeds the threshold value of 3×10^{19} Mx, the ephemeral region behaves like a small AR, following the Hale's and Joy's rules (Hagenaar et al. 2003). This explains the rotation of the tilt angle with respect to the solar east–west direction found in the *G*-band sequence. The observed slower westward velocity of the penumbral-like structure, which does not appear to follow the proper motion of the near sunspot, can be ascribed either to the generation of the ephemeral region by means of a local dynamo action or to the disconnection of the emerging bipole from the toroidal flux strand of the AR (Schrijver & Zwaan 2000). However, we cannot exclude other possibilities, such as moat flows around the sunspot.

Unfortunately, the simultaneous three-minute cadence longitudinal magnetograms taken in the Na I D1 line, present in the *Hinode* archive, began when the ephemeral region had already

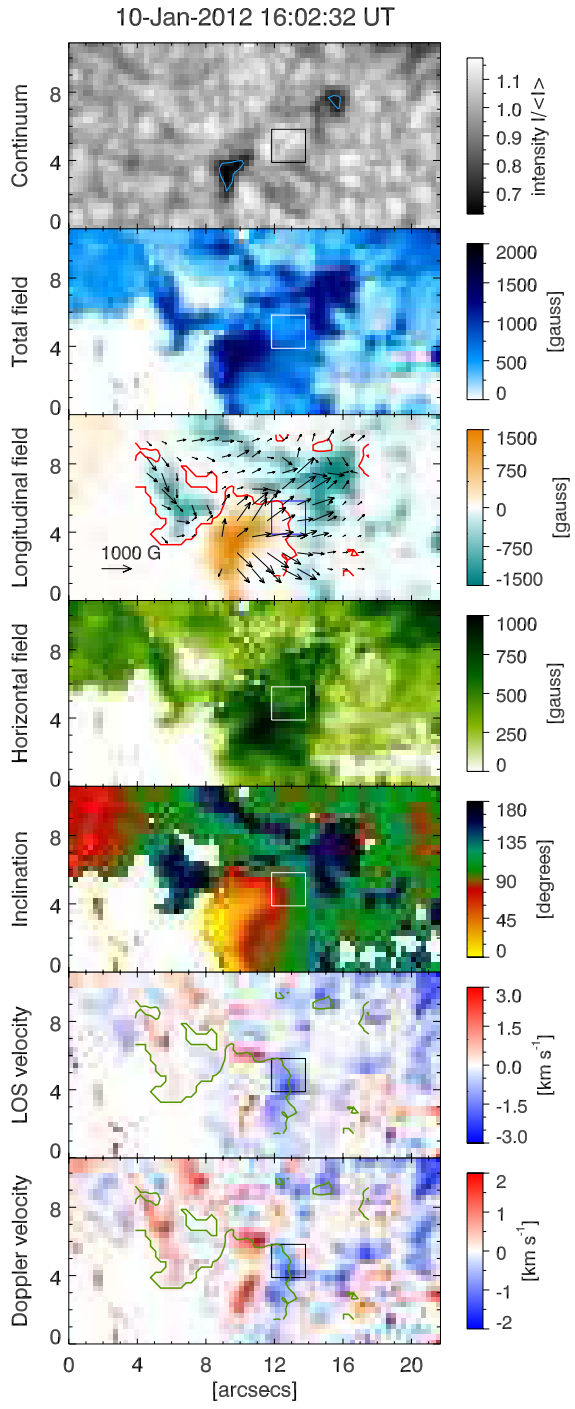

Figure 3. Maps showing the physical parameters of the penumbral-like structure, relevant to the data acquired by *Hinode* during the SOT/SP raster scan began at 15:34:08 UT. The subFoV is the same as that of the box shown in Figure 1. LOS velocity maps refer to results obtained from the M-E inversion, while Doppler velocity maps refer to the shifts deduced from the Fe I 630.15 nm line. The time refers to the acquisition time when the SOT/SP slit passed over the central position in the X direction of this subFoV. In the Fe I 630.2 nm line continuum intensity map, blue contours represent isophotes at $I_c = 0.7$. The emergence zone is indicated with a box. The red contour over the longitudinal field map (green over the velocity maps) represents the neutral line, with over plotted arrows indicating the transverse magnetic field. The white background represents pixels with total polarization $<1\%$, not considered.

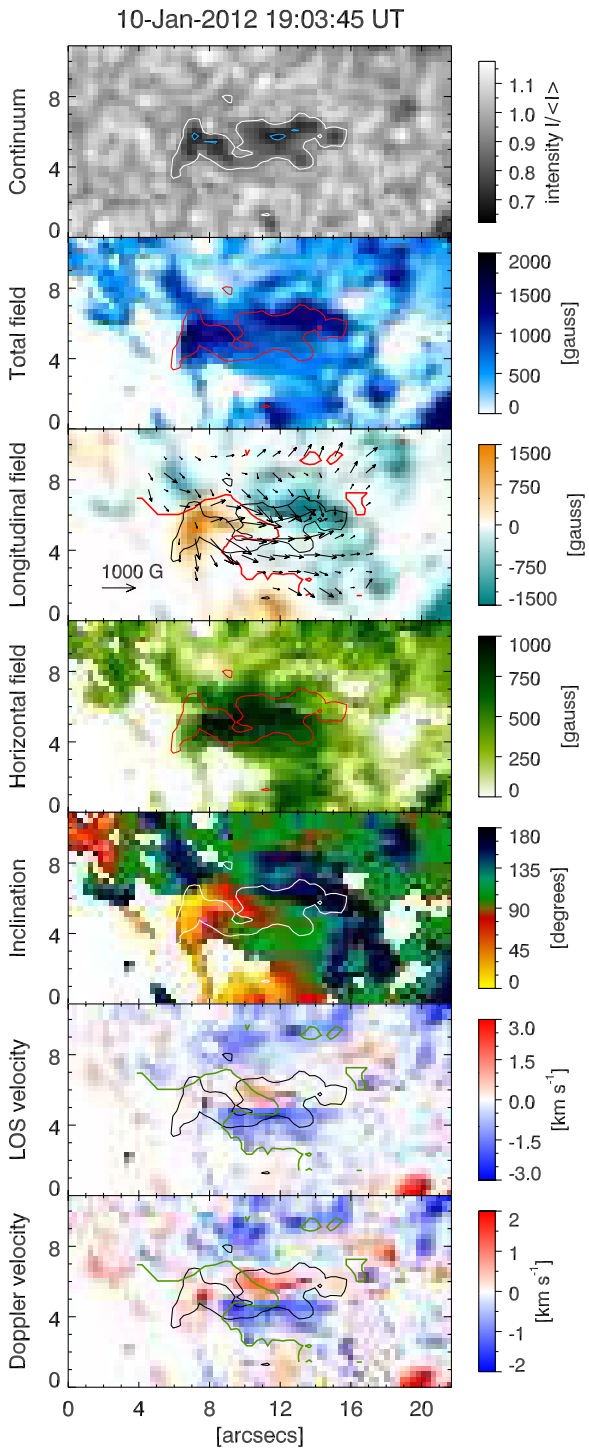

Figure 4. Same as in Figure 3, for the SOT/SP raster scan begun at 18:35:05 UT. The contours reproduced in the panels indicate isophotes at $I_c = 0.9$ (white color in the continuum intensity map).

appeared and were not able to follow the first stages of the emergence of the bipole.

Peculiar motions are found along the neutral line lying beneath these filaments, as Zuccarello et al. (2014) also found in another orphan penumbra. These motions are genuinely solar in their origin, as confirmed by Doppler shift maps. Although these observations are taken quite close to the disk center, the neutral line's change of position, produced by the transformation of the components of the vector magnetic field into the local solar frame, cannot allow us to find a one-to-one correspondence between pixels with intrinsic high horizontal field, nearly-zero vertical field, and high line-of-sight velocity values.

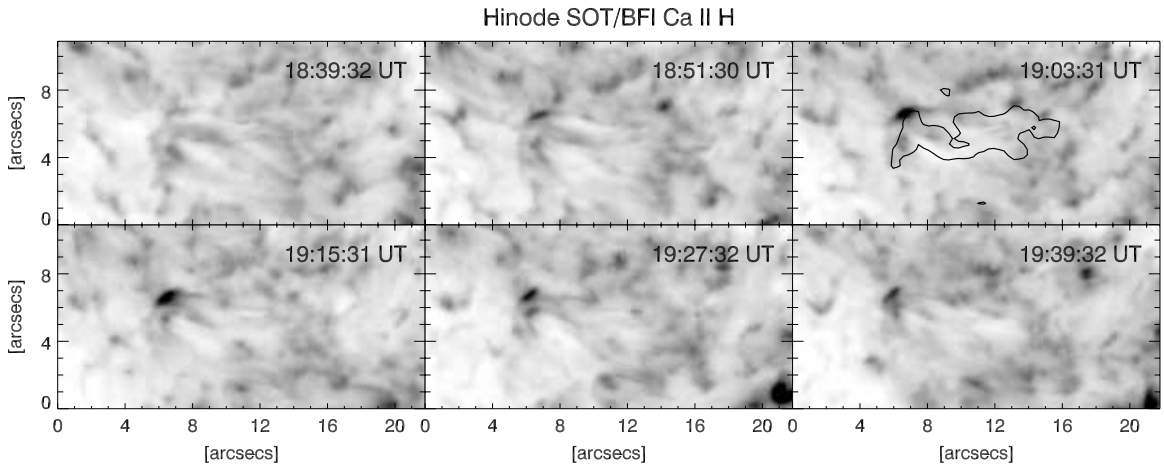

Figure 5. Sequence of SOT/FG Ca II H filtergrams for the same subFoV shown in Figure 2, in the interval 18:39–19:39 UT on January 10. Images are rescaled to the minimum and maximum intensity of the entire sequence, with reversed color scale. The contour refers to isophotes at $I_c = 0.9$ of the continuum intensity map of the simultaneous SOT/SP raster scan (see Figure 4).

In our observations, we find indirect confirmation of the presence of the magnetic canopy observed by Lim et al. (2013), as pointed out by the interaction between the positive patch of the emerging bipole and the plage negative field. The Ca II H brightening may be due to magnetic reconnection between these two flux systems (see, e.g., Guglielmino et al. 2008). The delay between the appearance of the positive emerging flux (before 15:37 UT) and the Ca II H brightness enhancement, at least 3.5 hr later, indicates that the interaction takes place between the emerging patch and fields lying at atmospheric levels higher than the Fe I 630.2 nm formation height. Taking into account the temperature response function of the SOT/BFI Ca II H filter deduced by Carlsson et al. (2007), the increase up to a factor of three in Ca II H intensity suggests that this phenomenon may take place in the upper photosphere or near the base of the chromosphere, given the absence of brightness enhancements in the simultaneous photospheric *G*-band image. The bright Hα patch seen almost simultaneously by Lim et al. (2013) is very likely to have the same origin as this Ca II H brightening.

Numerical simulations of photospheric flux emergence predict transient darkenings and anomalous granules with elongated intergranular lanes in correspondence of the emerging structures when the horizontal magnetic field is strong enough, i.e., above the equipartition value (Cheung et al. 2007, 2008, 2010; Tortosa-Andreu & Moreno-Insertis 2009). Elongated fibrilar dark alignments between flux concentrations aligned with the horizontal component of the emerging fields, interpreted as the top of the magnetic loops rising through the solar photosphere, are actually observed during flux emergence at different spatial scales (Wang & Zirin 1992; Strous & Zwaan 1999; Otsuji et al. 2007; Guglielmino et al. 2010).

Furthermore, three-dimensional MHD models of magneto-convection in inclined fields (see, e.g., Thomas & Weiss 2008) show a strong influence of the magnetic top boundary condition on penumbral formation. Penumbrae with larger radial extent are formed when the value of the horizontal field component increases (Rempel 2012). This is supported by chromospheric observations that indicate the presence of magnetic canopies before penumbral formation (Shimizu et al. 2012; Romano et al. 2013, 2014).

Our findings exclude that the penumbral-like structure is formed as a consequence of submerging horizontal fields because we find an emergence zone with upflow velocities of $\sim -1\,\mathrm{km\,s^{-1}}$.

For the target analyzed here, we should also rule out the scenario proposed by Kuckein et al. (2012a, 2012b), who interpreted an orphan penumbra as the photospheric counterpart of a filament observed in the chromosphere. The bottom part of this filament, still emerging but trapped in the photosphere, showed a strongly sheared configuration, with the field lines almost parallel to the polarity inversion line. Lim et al. (2013) already noticed that there was no evidence of a flux rope in their observations. Rather, they suggested the emergence of an Ω loop, though their data could not provide support for this guess, save the magnetic flux increase found in the region with *SDO*/HMI measurements. In fact, even we did not find evidence of a filament in the chromosphere above the region in simultaneous Big Bear Solar Observatory data.

In our SOT/SP data, the field lines in the emergence zone are almost orthogonal to the neutral line. The association of horizontal, normally oriented field lines and upflows definitively proves the Ω-shaped configuration of the emerging structure. Later, in the penumbral-like structure the magnetic configuration is more sheared.

We suggest that the combination of emerging horizontal fields and an overlying canopy can give rise to the penumbral-like filaments forming the observed structure. The horizontal part of the Ω loop remains trapped in the photosphere and, being the field stronger than the equipartition value, this leads to the formation of fibrilar dark alignments. The latter are favored to grow due to the presence of the canopy of the near sunspot. The evolution found in our analysis indicates that the penumbral-like filaments appear when the bipole has almost stopped emerging and its field lines float on the photosphere. Thus, the penumbral-like structure is the remnant of already emerged field lines, which receive positive feedback from the presence of the canopy and form filaments during some hours through magneto-convection in inclined fields. Since we find the ancestor of this structure, we would not name it as an *orphan penumbra*.

Hinode is a Japanese mission developed and launched by ISAS/JAXA, with NAOJ as a domestic partner and NASA and STFC (UK) as international partners. It is operated by these agencies in cooperation with ESA and NSC (Norway).

SOT/SP Inversions were conducted at NCAR under the framework of the Community Spectro-Polarimetric Analysis Center (CSAC; http://www.csac.hao.ucar.edu/). The authors thank the EC FP7/2007-2013 for financial support under the grant agreements eHEROES (project No. 284461) and SOLARNET (project No. 312495). This study was partially supported by the Università di Catania.

Facilities: Hinode (SOT), *SDO*

REFERENCES

Carlsson, M., Hansteen, V. H., de Pontieu, B., et al. 2007, PASJ, 59, 663
Cheung, M. C. M., Rempel, M., Title, A. M., & Schüssler, M. 2010, ApJ, 720, 233
Cheung, M. C. M., Schüssler, M., & Moreno-Insertis, F. 2007, A&A, 467, 703
Cheung, M. C. M., Schüssler, M., Tarbell, T. D., & Title, A. M. 2008, ApJ, 687, 1373
Denker, C., Zirin, H., & Wang, H. 1997, BAAS, 29, 901
Georgoulis, M. K. 2005, ApJL, 629, L69
Guglielmino, S. L., Bellot Rubio, L. R., Zuccarello, F., et al. 2010, ApJ, 724, 1083
Guglielmino, S. L., Zuccarello, F., Romano, P., & Bellot Rubio, L. R. 2008, ApJL, 688, L111
Hagenaar, H. J., Schrijver, C. J., & Title, A. M. 2003, ApJ, 584, 1107
Harvey, K. L., & Martin, S. F. 1973, SoPh, 32, 389
Jurčák, J., Bellot Rubio, L. R., & Sobotka, M. 2014, A&A, submitted
Kosugi, T., Matsuzaki, K., Sakao, T., et al. 2007, SoPh, 243, 3
Kuckein, C., Martínez Pillet, V., & Centeno, R. 2012a, A&A, 539, A131
Kuckein, C., Martínez Pillet, V., & Centeno, R. 2012b, A&A, 542, A112
Leka, K. D., & Skumanich, A. 1998, ApJ, 507, 454
Lim, E.-K., Yurchyshyn, V., Goode, P., & Cho, K.-S. 2013, ApJL, 769, L18
Lites, B. W., Skumanich, A., & Martínez Pillet, V. 1998, A&A, 333, 1053
Otsuji, K., Shibata, K., Kitai, R., et al. 2007, PASJ, 59, 649
Pesnell, W. D., Thompson, B. J., & Chamberlin, P. C. 2012, SoPh, 275, 3
Rempel, M. 2011, ApJ, 729, 5
Rempel, M. 2012, ApJ, 750, 62
Rempel, M., & Schlichenmaier, R. 2011, LRSP, 8, 3
Rempel, M., Schüssler, M., Cameron, R. H., & Knölker, M. 2009, Sci, 325, 171
Romano, P., Frasca, D., Guglielmino, S. L., et al. 2013, ApJL, 771, L3
Romano, P., Guglielmino, S. L., Cristaldi, A., et al. 2014, ApJ, 786, 10
Schlichenmaier, R. 2009, SSRv, 144, 213
Schou, J., Scherrer, P. H., Bush, R. I., et al. 2012, SoPh, 275, 229
Schrijver, C. J., & Zwaan, C. 2000, Solar and Stellar Magnetic Activity (Cambridge Astrophysics Series, Vol. 34; New York: Cambridge Univ. Press)
Shimizu, T., Ichimoto, K., & Suematsu, Y. 2012, ApJL, 747, L18
Shimizu, T., Katsukawa, Y., Matsuzaki, K., et al. 2007, PASJ, 59, 845
Strous, L. H., & Zwaan, C. 1999, ApJ, 527, 435
Thomas, J. H., & Weiss, N. O. 2008, Sunspots and Starspots (Cambridge: Cambridge Univ. Press)
Tortosa-Andreu, A., & Moreno-Insertis, F. 2009, A&A, 507, 949
Tsuneta, S., Ichimoto, K., Katsukawa, Y., et al. 2008, SoPh, 249, 167
Wang, H., & Zirin, H. 1992, SoPh, 140, 41
Zirin, H., & Wang, H. 1991, AdSpR, 11, 225
Zuccarello, F., Guglielmino, S. L., & Romano, P. 2014, ApJ, submitted